RAPID COMMUNICATIONS

PHYSICAL REVIEW E VOLUME 48, NUMBER 5 NOVEMBER 1993

Wave-breaking limit to the wake-field effect in an underdense plasma

Denis Teychenné and Guy Bonnaud

Commissariat à l'Energie Atomique, Centre d'Etudes de Limeil-Valenton, 94195 Villeneuve St. Georges, France

Jean-Louis Bobin

Université Pierre et Marie Curie, Tour 13, E5, 75252 Paris, France

(Received 8 January 1993)

The influence of the sub-light-speed group velocity of a square-shaped laser pulse on a longitudinal wake-field wave is examined via a one-dimensional analysis of the electric potential equation. Analytical expressions for the potential, the electric field, the wake-field wavelength, and the optimum pulse width are obtained and fully agree with results from the numerical integration of the potential equation. The conditions for the onset of wave breaking due to sub-light-velocity pulses are given for both leading and trailing pulse edges, in agreement with particle simulations.

PACS number(s): 52.35.Mw, 52.40.Db, 52.35.Fp, 52.40.Nk

Recently, compact terawatt lasers within the wavelength range 0.25–1.05 μm have been able to deliver, after focusing, irradiances up to 10^{18} W/cm^2 [1]. This gives the focal-volume electrons a relativistic quiver momentum, which, normalized to $m_e c$, is written as $a_0=0.85(I_0\lambda_0^2/10^{18})^{1/2}$, where m_e denotes the electron mass, c is the light velocity in vacuum, λ_0 is the laser wavelength in micrometers, and I_0 is the laser irradiance in units of W/cm^2. The electron motion is largely influenced by the ponderomotive force associated with the longitudinal gradient of the laser pulse energy (along the pulse propagation). This force gives rise, behind the laser pulse, to a coherent motion of the electron fluid in the form of an electron plasma wave (EPW); this is the so-called wake-field effect. A large electric field with a phase velocity equal to the laser group velocity can be induced; this may turn out to be of great interest as a new electron-accelerator concept.

During the past years this effect has been intensively studied via a single-electron-fluid model within the assumption $v_g=c$ [2,3]. In this paper, we remove this assumption and we address the influence of the laser group velocity on the various wake-field EPW features and, especially, we consider the limit to the EPW generation. Beyond a critical irradiance, the longitudinal velocities of some electrons are so large that they are predicted to exceed the finite propagation velocity (group velocity) of the laser light. Electron overtaking then results and induces EPW breaking with fast-electron generation, thus nullifying further application of the single-fluid model.

The plasma is assumed to be cold, homogeneous with density n_0, electrically neutral, and having immobile ions. The laser wave is a planar wave, the group velocity of which is assumed to be constant over the pulse. Although the group-velocity modification from its classical value due to relativistic effects is still not well understood, the latter assumption is valid if the pulse is about one electron-plasma-period wide and propagates over a few pulse lengths. Along the longitudinal direction denoted by x, the laser-plasma interaction is described by the electron density n_e, velocity v_x, and the electric potential ϕ, which are coupled by the density and momentum conservation equations and the Poisson equation. In a frame drifting with velocity v_g with respect to the laboratory frame, and by using the so-called quasistatic approximation (QSA) [2], which assumes no feedback of the EPW onto the laser wave, the basic equations [2] simplify to

$$\frac{n_e}{n_0}(\beta_g-\beta_x)=\beta_g \ , \tag{1a}$$

$$\gamma(1-\beta_g\beta_x)=1+\tilde{\phi} \ , \tag{1b}$$

$$\frac{\partial^2\tilde{\phi}}{\partial\zeta^2}=\frac{n_e}{n_0}-1 \ , \tag{1c}$$

with $\zeta=(\omega_{pe}/c)(x-v_g t)$, where t denotes time, $\beta_g=v_g/c$, $\beta_x=v_x/c$, and $\tilde{\phi}=e\phi/m_e c^2$, and ω_{pe} is the electron plasma frequency. γ is the electron Lorentz factor $\gamma_\perp(1-\beta_x^2)^{-1/2}$ with $\gamma_\perp^2=1+\alpha_0^2/2f(\zeta)$; f denotes the energy profile of their incident laser pulse and $\alpha=1$ or 2 for linear or circular laser polarization, respectively; $-e$ is the electron charge; the unperturbed-plasma frequency satisfies $\omega_{pe}/\omega_0<1$, since we consider underdense plasma (ω_0 is the radial laser frequency). Defining $\psi=1+\tilde{\phi}$ and combining Eqs. (1a)–(1c) yield the nonlinear equation

$$\frac{\partial^2\psi}{\partial\zeta^2}=\frac{\beta_g\gamma_\perp^2-\psi[\psi^2-\gamma_\perp^2(1-\beta_g^2)]^{1/2}}{\beta_g(\psi^2-\gamma_\perp^2(1-\beta_g^2))+\psi[\psi^2-\gamma_\perp^2(1-\beta_g^2)]^{1/2}} \ . \tag{2}$$

Under the assumption $\beta_g=1$, Eq. (2) reduces to the expression $\partial^2\psi/\partial\zeta^2=\frac{1}{2}(\gamma_\perp^2/\psi^2-1)$, which is identical to the Eq. (6b) result of Esarey and co-workers [2]. In the general classical regime $\beta_g\neq 1$, $a_0\ll 1$, Eq. (2) reduces to a forced harmonic oscillator equation $\beta_g^2\partial^2\tilde{\phi}/\partial\zeta^2+\tilde{\phi}=\alpha a_0^2 f(\zeta)/4$, which is the basic equation of Gorbunov and Kirzanov's paper [4].

To prevent complex values in Eq. (2), the potential needs to exceed a minimum potential $\tilde{\phi}_{md}=\psi_{md}-1$ given by

$$\psi_{md}\equiv\gamma_\perp\sqrt{1-\beta_g^2} \ , \tag{3}$$

where the index *md* denotes *minimum* and *destruction*. From Eq. (1b) and the γ definition, we can observe that $\psi\rightarrow\psi_{md}$ also implies $\beta_x\rightarrow\beta_g$; the onset of complexity

thus signals the failure of the fluid approximation due to electron overtaking and thus denotes wave breaking. Equation (3) may be verified either inside the pulse if $\psi \geq \gamma_0(1-\beta_g^2)^{1/2}$ or at the trailing edge if $\psi \geq (1-\beta_g^2)^{1/2}$, where γ_0 denotes $\gamma_\perp > 1$. This irradiance-dependent limit is due to the increase in the electron inertial mass, causing a lower-electron velocity inside the pulse. For $\zeta=0$, ψ is minimum and equals 1; for a square pulse this gives the wave-breaking condition $\gamma_0 \leq 1/(1-\beta_g^2)^{1/2}$ (see the top curve in Fig. 1).

Henceforth, we assume a square-shaped pulse: $f(\zeta)=1$, $\gamma_\perp=\gamma_0$ for $-\zeta_0 \leq \zeta \leq 0$ and $f(\zeta)=0$, $\gamma_\perp=1$ for $\zeta \leq -\zeta_0$. In contrast to other pulse shapes, this approximation lets us separate the variables ψ and ζ in Eq. (2) and integrate once to obtain

$$\left[\frac{d\psi}{d\zeta}\right]^2 = -\frac{\gamma_\perp^2(1+\beta_g)}{\psi+[\psi^2-\gamma_\perp^2(1-\beta_g^2)]^{1/2}} - \frac{\psi+[\psi^2-\gamma_\perp^2(1-\beta_g^2)]^{1/2}}{1+\beta_g} + C_{1,2} , \quad (4)$$

with the constants $C_{1,2}$ determined by the domain of interest, i.e., the pulse (C_1) and the pulse wake (C_2). If we rewrite Eq. (4) as $(d\psi/d\zeta)^2 = F(\psi,\gamma_\perp,\beta_g)+C_{1,2}$, the requirement for continuity of ψ and $d\psi/d\zeta$ at the front edge ($\zeta=0$) gives $C_1 = -F(1,\gamma_0,\beta_g)$ and, at the rear edge ($\zeta=-\zeta_0$), gives $C_2 = F(\psi(-\zeta_0),\gamma_0,\beta_g) - F(\psi(-\zeta_0),1,\beta_g) - F(1,\gamma_0,\beta_g)$.

We now consider the solutions to Eq. (4) inside the pulse. An integral expression for ζ is obtained, which, by defining $U=\psi+[\psi^2-\gamma_0^2(1-\beta_g^2)]^{1/2}$, becomes

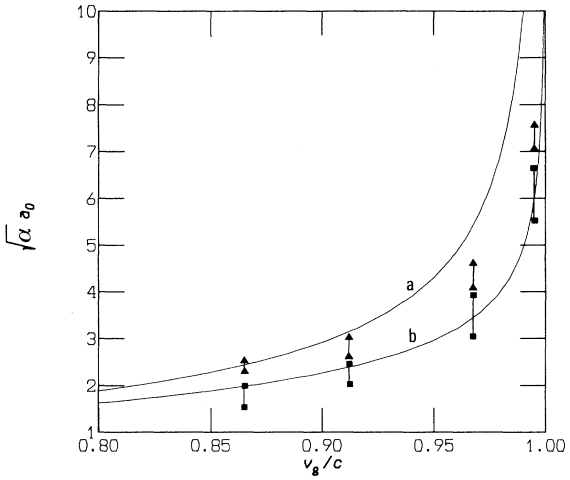

FIG. 1. Critical laser electric field $\sqrt{\alpha}a_0$ for wave breaking onset vs the laser group velocity. The curves labeled *a* and *b* correspond to the pulse and the wake-field regions, respectively. The incident electric fields a_0, which induce wave breaking in both particle simulations and direct numerical solution of the potential equation are framed by bars; the latter are terminated by squares for a square pulse, the full width of which is $\zeta_0=\pi$, and by triangles for a sine-squared pulse with $\zeta_0=2\pi$. The classical expression for the group velocity $v_g/c=(1-\omega_{pe}^2/\omega_0^2)^{1/2}$ is used for $\omega_{pe}/\omega_0=0.5$, 0.41, 0.25, and 0.1. The conditions associated with the bottom squares and triangles do not exhibit wave breaking, in contrast to the top ones.

$$\zeta = -\sqrt{1+\beta_g}\left\{\sqrt{U_+}\left[1-\gamma_0^2\frac{(1-\beta_g^2)}{U_+U_-}\right]E(\chi_1,m_1) - \left[\frac{U_+-U)(U-U_-)}{U}\right]^{1/2}\right\} . \quad (5)$$

E denotes the elliptic integral of the second kind [5], where its argument χ_1, its modulus m_1, and the quantities $U_\pm$ are defined as

$$\chi_1 = \sin^{-1}\left[\frac{U_+(U-U_-)}{(U_+-U_-)U}\right]^{1/2} , \quad m_1 = \left[1-\frac{U_-}{U_+}\right]^{1/2} \quad (6)$$

$$U_+ = \frac{(1+\beta_g)^2\gamma_0^2}{1+[1-\gamma_0^2(1-\beta_g^2)]^{1/2}} ,$$
$$U_- = 1+[1-\gamma_0^2(1-\beta_g^2)]^{1/2} . \quad (7)$$

Real solutions require that $U_- \leq U \leq U_+$. For $U=U_+$, which corresponds to the maximum potential, $\chi_1=\pi/2+n\pi$ (n is an integer) and the elliptic integral E is complete. This value of χ_1 lets us define the optimum pulse length as $(2n+1)\zeta_{op}$ with

$$\zeta_{op} = 2\gamma_0\beta_g\left[\frac{1+\beta_g}{1+[1-\gamma_0^2(1-\beta_g^2)]^{1/2}}\right]^{1/2} E\left[\frac{\pi}{2},m_1\right] . \quad (8)$$

Figure 2 shows the evolution of ζ_{op} as a function of β_g. For low values of a_0, the classical result is recovered [4], i.e., the pulse width is at least one-half of the wake-field EPW wavelength, $\zeta_{op}=\pi v_g/c$. For $\zeta=-\zeta_{op}$, we have $U=U_+$, giving the maximum electric potential,

$$\tilde{\phi}_M = 2\beta_g\left[\frac{\gamma_0^2}{1+[1-\gamma_0^2(1-\beta_g^2)]^{1/2}} - \frac{1}{1+\beta_g}\right] . \quad (9)$$

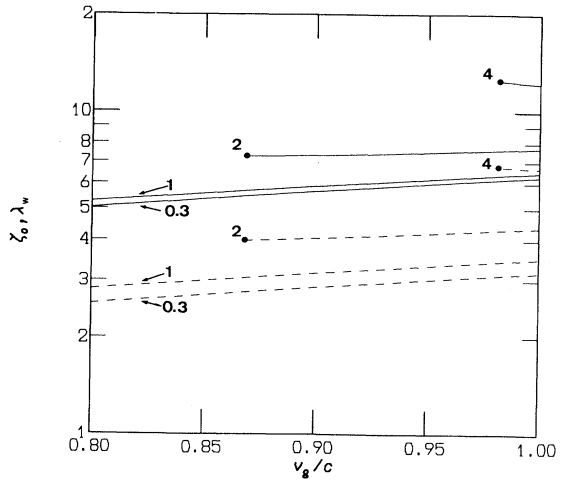

FIG. 2. Optimal pulse length (dotted lines) maximizing the electric potential and wavelength (full lines) of the wake plasma wave vs the laser group velocity. The curves are labeled with the values of $\sqrt{\alpha}a_0$.

The smallest potential value given by $U=U_-$ is simply $\tilde{\phi}=0$. The normalized electric field $\tilde{E}\equiv e/m_e\omega_{pe}c$ can be expressed as $\tilde{E}=-d\psi/d\zeta$ and therefore is maximum when Eq. (2) $=0$; this yields $\psi=\gamma_0$ and, using Eq. (4), this gives the maximum (M) and minimum (m) electric fields,

$$\tilde{E}_M=-\tilde{E}_m=\sqrt{2}\left[-\gamma_0+\frac{1}{1+\beta_g}+\frac{\gamma_0^2\beta_g}{1+[1-\gamma_0^2(1-\beta_g^2)]^{1/2}}\right]^{1/2}. \quad (10)$$

The previous results [2] are recovered when $\beta_g=1$. Inside the pulse, we have $C_1=\gamma_0^2+1$, $U_+=2\gamma_0^2$, $U_-=2$, and $U=2\psi$. Then the optimum pulse length becomes $\zeta_{\rm op}=2\gamma_0 E(\pi/2,m_1)$, with $m_1=(1-1/\gamma_0^2)^{1/2}$, and the maximum potential and electric field given by $\tilde{\phi}_M=\gamma_0^2-1$ and $\tilde{E}_M=\gamma_0-1$, respectively.

Now we deal with the wake field itself, behind the pulse, in the case of the optimum pulse length. As seen above, the potential is then maximum at the end of the pulse, leading to $C_2=-F(\psi(-\zeta_0),1,\beta_g)$. If we denote $X=\psi+[\psi^2-(1-\beta_g^2)]^{1/2}$, we obtain as the solution of Eq. (4):

$$\zeta=-(2n+1)\zeta_{\rm op}-\sqrt{1+\beta_g}\left\{\sqrt{X_+}\left[1-\frac{1-\beta_g^2}{X_+X_-}\right]\times E(\chi_2,m_2)+\frac{1-\beta_g^2}{X_-\sqrt{X_+}}\left[\frac{(X_+-X)(X-X_-)}{X_+}\right]^{1/2}\right\}, \quad (11)$$

where the argument χ_2, the modulus m_2 of the elliptic integral, and the variables $X_\pm$ are

$$\chi_2=\sin^{-1}\left[\frac{X_+-X}{X_+-X_-}\right]^{1/2},\quad m_2=\left[1-\frac{X_-}{X_+}\right]^{1/2},\quad X_\pm=\frac{1+\beta_g}{2}(C_2\pm\sqrt{C_2^2-4}). \quad (12)$$

The variable X must lie in the range $[X_-,X_+]$. The locations where $\chi_2=n\pi$ are associated with $X=X_+$, i.e., the maximum potential, and the locations where $\chi_2=\pi/2+n\pi$ are associated with $X=X_-$, i.e., the minimum potential. Unfortunately, the resulting expressions cannot be reduced to compact expressions like those for ψ inside the pulse. Behind the pulse, a spatially periodic pattern appears with the following wavelength:

$$\lambda_w=2\sqrt{1+\beta_g}\sqrt{X_+}\left[1-\frac{1-\beta_g^2}{X_+X_-}\right]E\left[\frac{\pi}{2},m_2\right], \quad (13)$$

whose dependence on β_g and a_0 is displayed in Fig. 2; the wake-field wavelength is roughly twice the optimum length. Inside the wake field, the maximum potential is given by Eq. (9) and the minimum potential by

$$\tilde{\phi}_m=\frac{1}{2}\left[\frac{(1+\beta_g)^2}{X_+}+X_+\frac{1-\beta_g}{1+\beta_g}\right]-1, \quad (14)$$

where we can use $X_+=\psi_M+\sqrt{\psi_M-(1-\beta_g^2)}$. From Eq. (2) with $\gamma_\perp=1$, we can observe that the electric field is maximized or minimized for $\psi=1$, i.e., $X=1+\beta_g$. Substituting $\psi=1$ in Eq. (4) yields for the minimum and maximum fields

$$\tilde{E}_M=-\tilde{E}_m=\sqrt{2}\left[\frac{\beta_g}{\psi_M+[\psi_M^2-(1-\beta_g^2)]^{1/2}}+\frac{\psi_M}{1+\beta_g}-1\right]^{1/2}. \quad (15)$$

For $\beta_g=1$, we recover the previous results [2]. Indeed, we have $C_2=1/\gamma_0^2+\gamma_0^2$, so that the potential oscillates between $\tilde{\phi}_m=-1+1/\gamma_0^2$ and $\phi_M=\gamma_0^2-1$ and the wake-field wavelength becomes $\lambda_w=4\gamma_0 E(\pi/2,m_2)$, with $m_2=(1-1/\gamma_0^4)^{1/2}$; the maximum electric field reduces to $\tilde{E}_M=\gamma_0-1/\gamma_0$. As shown by Fig. 3, $\tilde{\phi}_M$ and $\tilde{E}_M$ increase with decreasing β_g; the larger the irradiance, the stronger the increase. The dotted lines indicate the wave breaking limit described in the next paragraph; they let us observe that the permitted group velocity range narrows dramatically with increasing irradiance.

At this point, we can express more clearly the wave-breaking condition, Eq. (3). Indeed, the latter leads to $\psi_m=(1-\beta_g^2)^{1/2}$, which, in Eq. (14), yields a relation between X_+ and β_g. We subsequently find the maximum laser irradiance beyond which the wake-field EPW breaks:

$$\gamma_{0d}^2=\frac{1+\beta_g^2}{4\beta_g^2}\left[\left[\frac{(1+\beta_g)^3}{1-\beta_g}\right]^{1/2}+\left[\frac{(1-\beta_g)^3}{1+\beta_g}\right]^{1/2}-\frac{2}{1+\beta_g^2}-\beta_g^2\right]. \quad (16)$$

When β_g approaches 1, γ_{0d}^2 scales as $\sqrt{2/(1-\beta_g)}$. The dependence of γ_{0d} vs β_g is given by the bottom curve in Fig. 1, which lies clearly below the wave-breaking condition inside the pulse. At wave breaking, Eq. (15) gives the maximum electric field:

$$\tilde{E}_{Md}=\sqrt{2}\left[\frac{1}{(1-\beta_g^2)^{1/2}}-1\right]^{1/2}, \quad (17)$$

which expression is exactly Akhiezer and Polovin's prediction [6], since the EPW phase velocity is equal to the laser-group velocity.

The analytic expressions derived above, which have been set forth, have been spot checked by numerical solutions of the potential equation, Eq. (2), via a fourth-order Runge-Kutta scheme. As an example, Fig. 4 displays the electric field along z for two different β_g and the associated optimum pulse lengths: as β_g decreases approaching the wave-breaking limit, the wave clearly steepens. A typical feature of the optimum pulse is that the longitudinal electric field is zero and the potential is maximum at the end of the pulse; as a consequence, ψ is a monotonic function of z inside an optimum pulse. We stress that the numerical check of wave-breaking onset requires very small mesh size and that too large a mesh size provides a smaller threshold for a_0; so, the mesh size $\Delta\zeta=2\pi/400$ for $\beta_g=0.995$ gives a complex solution at the theoretical

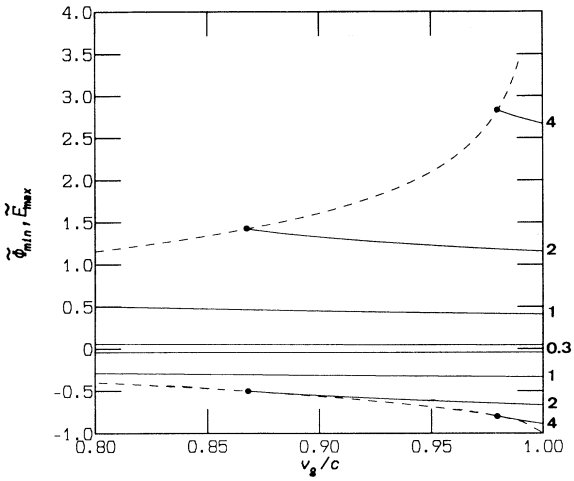

FIG. 3. Minimum potential (below 0) and maximum electric field (above 0) for the EPW inside the wake field vs the laser-group velocity (full lines): the curves are labeled with the values of $\sqrt{\alpha}a_0$. Same quantities at wave breaking (dotted lines).

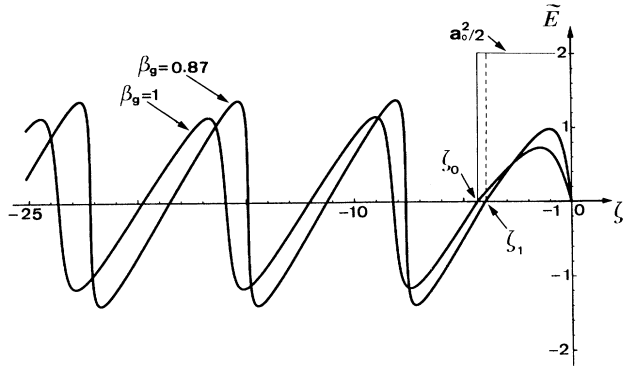

FIG. 4. Electric field $\tilde{E}$ vs space $\zeta=x\omega_{pe}/c$ obtained by numerical solving of the EPW potential equation for the group velocities $v_g/c=1$ and 0.87; the pulse length is optimum. The laser field is $\sqrt{\alpha}a_0=2$ and the laser pulse propagates from left to right.

value $a_0=6$, whereas a doubled mesh size gives $a_0=5$.

Using the $1\frac{1}{2}$-dimensional relativistic particle-in-cell computer code EUTERPE, we looked for the conditions under which some electron orbits distinctly cross each other and the EPW electric field reaches Akhiezer and Polovin's limit E_{Md}, behind the pulse. We have chosen four distinct plasma densities and compare in Fig. 1 the results with the analytical ones by using the classical group velocity $v_g/c=(1-\omega_{pe}^2/\omega_0^2)^{1/2}$. Both the square pulse and the more realistic sine-squared shaped pulse defined by $f(0<\zeta<\zeta_0)=\sin^2(\pi\zeta/\zeta_0)$ with $\zeta_0=2\pi$ and $f(\zeta>\zeta_0)=0$ were used. As previously seen by Watteau *et al.* [1], the pulse width has less effect than for classical irradiances, so that the optimum pulse width is not sharply defined. The bars in Fig. 1 represent incident field ranges; for the bottom values, no crossing of electron orbits is observed and, for the top values, electron overtaking and the amplitude E_{Md} for the electric field at the trailing pulse edge are observed; the squares indicate a square profile and lie below the triangles which are associated with a sine-squared profile. The close agreement of the "bars with squares" with Eq. (16) indicates that the laser-pulse modification does not play a role before wave breaking, which is consistent with our assumption of a given group velocity; wave breaking takes place immediately after the pulse. We find that the bell-shaped pulses give rise to wave breaking for slightly larger irradiance ranges; this is consistent with the fact that the maximum potential for a bell-shaped pulse is somewhat smaller than the one for a square pulse, according to numerical results from the potential equation integration. As a general rule for the relativistic regime, the sharper the leading pulse edge, the stronger the wake-field EPW; the square pulse is therefore the most efficient profile, and the bell-shaped profile does not depart greatly from the former if the pulse width is about the same as or smaller than $2\pi/\omega_{pe}$. Wave breaking leads to very fast electrons: at $0.01n_c$, a $40\lambda_0$-long plasma gave at $a_0=6$ electron energies up to 17 MeV. Such large energies are due to the subsequent acceleration by the EPW field of the electrons ejected from the wave-breaking region.

As a conclusion, taking into account the sub-light-laser group velocity brings limits to the transfer of the laser-pulse energy to a coherent EPW. This means that, for a given density, increasing the irradiance above the threshold presented in this paper would break the EPW and would lead to fast electron generation. We have provided a simple analytic criterion for the wave-breaking onset. Inside the pulse, the EPW is stabilized and can lead to electric fields much larger that the usual isolated-EPW limit.

Note added. We recently became aware of a paper on the wake field induced by sub-light-speed pulses: I. G. Murusidze and L. N. Tsintsadze, J. Plasma Phys. **48**, 391 (1992).

One of the authors (G.B.) acknowledges fruitful conversations with E. Esarey, W. Mori, J. M. Rax, and D. Umstadter.

[1] P. Maine, D. Strickland, P. Bado, M. Pessot, and G. Mourou, IEEE J. Quant. Electron. **24**, 398 (1988); M. Ferray, L. A. Lompré, O. Gobert, G. Mainfray, C. Manus, A. Sanchez, and A. Gomes, Opt. Commun. **75**, 278 (1990); M. D. Perry, F. G. Patterson, and J. Weston, Opt. Lett. **15**, 381 (1990); J. P. Watteau, G. Bonnaud, J. Coutant, R. Dautray, A. Decoster, M. Louis-Jacquet, J. Ouvry, J. Sauteret, S. Seznec, and D. Teychenné, Phys. Fluids B **4**, 2217 (1992).

[2] P. Sprangle, E. Esarey, and A. Ting, Phys. Rev. A **41**, 4463 (1990); Phys. Rev. Lett. **64**, 2011 (1990); V. I. Berezhiani and I. G. Murusidze, Phys. Lett. A **148**, 338 (1990).

[3] J. M. Rax and N. Fisch, Phys. Fluids B **4**, 1323 (1992).

[4] L. M. Gorbunov and V. I. Kirsanov, Zh. Eksp. Teor. Fiz. **93**, 509 (1987) [Sov. Phys. JETP **66**, 290 (1987)].

[5] I. S. Gradhshteyn and I. M. Ryzhik, *Table of Integrals, Series and Products* (Academic, London, 1980).

[6] A. I. Akhiezer and R. V. Polovin, Zh. Eksp. Teor. Fiz. **30**, 915 (1956) [Sov. Phys. JETP **3**, 696 (1956)]; W. B. Mori and T. Katsouleas, Phys. Scr. **T30**, 127 (1990).